Journal of Marine Research, 58, 863–894, 2000

Relative dispersion in the subsurface North Atlantic

by J. H. LaCasce[1] and A. Bower[1]

ABSTRACT

Pair statistics are calculated for subsurface floats in the North Atlantic. The relative diffusivity (the derivative of the mean square particle separation) is approximately constant at large scales in both eastern and western basins, though the implied scale of the energy-containing eddies is greater in the west. But the behavior at times soon after pair deployment is quite different in the two basins; in the west the diffusivity grows approximately as distance to the 4/3 power, consistent with an inverse turbulent cascade of energy (or possibly of mixing superimposed on a mean shear), but in the east the diffusivity grows more slowly, as for instance in simple stochastic systems. Exponential stretching, expected in an enstrophy cascade, is not resolved in any region; however, this may reflect only that the present pair separations are too large initially.

1. Introduction

A patch of marked fluid advected in a turbulent flow generally undergoes a complex evolution, translating and distorting as it goes. In general it is difficult or impossible to predict such an evolution, so researchers have long recognized that the most sensible description of turbulent diffusion is a statistical one.

A complete statistical description of turbulent diffusion requires knowing the probability that marked fluid at a given time can be found simultaneously at n points in space (Batchelor and Townsend, 1953). The case with $n = 1$ concerns "absolute" or "single particle" statistics and relates to the translation of marked fluid; the case with $n = 2$ concerns "relative" statistics and relates to distortion. In practice, one quantifies the $n = 1$ and $n = 2$ statistics using single particles and pairs of particles, respectively. And while higher order moments are also possible (requiring triads of particles, and so on), the first two are the most accessible with typical geophysical data sets.

Under a variety of conditions, the absolute dispersion (the mean square particle displacement from its starting position) exhibits generic tendencies (Batchelor and Townsend, 1953): it increases quadratically in time initially and linearly in time after the Lagrangian integral time (Taylor, 1921; Batchelor and Townsend, 1953; Babiano *et al.,* 1987; Rupolo *et al.,* 1996), implying a constant diffusivity (the time derivative of the dispersion) after the integral time; in such cases, the diffusivity is said to "exist." Oceanic float data are most often analyzed in terms of absolute statistics, in particular to determine regional means, variances and diffusivities (e.g. Davis, 1991).

1. Woods Hole Oceanographic Institution, Woods Hole, Massachusetts, 02543, U.S.A. ***email: jlacasce@whoi.edu***

Relative (pair) dispersion is harder to predict *a priori*. Particles deployed close together generally separate on average, but the rate of separation often depends on the magnitude of the separation itself. Fluid dynamicists recognized that this latter fact is actually advantageous because relative dispersion can in principle shed light on the physics at different scales. Relative dispersion is much less familiar in the oceanic context than is absolute dispersion, and we have little idea of how pairs of floats ought to behave.

A broad overview of the theoretical predictions for two particle statistics and of existing observations is given by Bennett (1987). Babiano *et al.* (1990) discuss relative dispersion in the context of two-dimensional turbulence, with numerical results to illustrate different types of behavior. A brief overview of the various predictions are presented in the following section, but for more detail the reader is referred to the aforementioned works.

a. Theoretical expectations

Early theoretical work on pair statistics exploited turbulence theory. In turbulence, energy *cascades* to different scales: to smaller scales in three dimensions and to larger scales in two (e.g. Batchelor, 1960). If one assumes the rate of energy transfer between source and sink (dissipation) is constant (Kolmogorov, 1941) and further that the turbulence is homogeneous and isotropic, dimensional arguments (Batchelor, 1952) suggest a relative diffusivity:

$$K^{(2)} \equiv \frac{1}{2}\frac{d}{dt}\langle D^2\rangle = \varepsilon t^2 f\left(\frac{D_0}{\varepsilon^{1/2}t^{3/2}}, \frac{t\varepsilon^{1/2}}{\nu^{1/2}}\right) \tag{1}$$

where $\langle D^2\rangle$ is the mean square particle separation over an ensemble of pairs, t the time since pair deployment, D_0 the initial separation and ε the energy dissipation rate (with units L^2/T^3). With 3D turbulence, ν is a molecular viscosity. At scales greater than those where dissipation occurs, that is in the so-called energy "inertial" range, the diffusivity is presumedly independent of ν, yielding $f = f(D_0/\varepsilon^{1/2}t^{3/2})$.

Soon after deployment, particles separate with an approximately constant velocity (imagine a Taylor expansion in space of the Eulerian velocity), which implies the mean square separation increases quadratically and the diffusivity linearly in time. Then (1) reduces to:

$$K^{(2)} \propto t(\varepsilon D_0)^{2/3}. \tag{2}$$

Later on the dependence on the initial separation will be lost, so that $f = const.$ and $K^{(2)} \propto \varepsilon t^2$, or:

$$K^{(2)} \propto \varepsilon^{1/3}(\langle D^2\rangle)^{2/3}. \tag{3}$$

This is the well-known "4/3 law," deduced originally by Richardson (1926), as discussed below.

Alternately, one can measure the mean square separation velocity; in the asymptotic limit at which the dependence on D_0 is lost, this is:

$$\left\langle \left| \frac{dD}{dt} \right|^2 \right\rangle \propto \varepsilon t. \tag{4}$$

In 3D turbulence there is only the energy cascade, but in 2D turbulence there is a simultaneous cascade to smaller scales of *enstrophy* (or vorticity squared; Kraichnan, 1967; Batchelor, 1969). Assuming the enstrophy transfer rate is constant and equal to the dissipation rate, the diffusivity is:

$$K^{(2)} \propto \eta^{2/3} t \langle D_0^2 \rangle, \tag{5}$$

soon after deployment, and

$$K^{(2)} \propto \eta^{1/3} \langle D^2 \rangle, \tag{6}$$

after the dependence on the initial separation has been lost (Kraichnan, 1966; Lin, 1972; Bennett, 1987; Babiano *et al.,* 1990). Here η is the enstrophy dissipation rate, with dimensions of $1/T^3$. The fact that η is independent of the length scale yields an essential difference with the energy cascade case in the long time limit; however, with both types of cascade, the initial temporal growth of the diffusivity is linear.

Eq. (6) implies an *exponential* growth of particle separations:

$$\langle D^2 \rangle \propto \exp(\eta^{1/3} t) \tag{7}$$

and a similar growth in the mean square relative velocities. Again, such growth occurs in the asymptotic limit in which D_0 is forgotten, which means it can be hard to observe (Babiano *et al.,* 1990; Sec. 4b(ii)). Incidentally, exponential divergence is a well-known feature of chaotic flows (e.g. Guckenheimer and Holmes, 1983).

Ultimately, pair separations reach the scale of the energy-containing eddies, L_E, and the individual particle velocities become uncorrelated. Assuming homogeneity, the mean square relative velocities then are just twice the mean square particle velocities, for instance in the zonal direction:

$$\left\langle \left| \frac{dD_1}{dt} \right|^2 \right\rangle = \langle (u_i - u_j)^2 \rangle = \langle u_i^2 \rangle - 2\langle u_i u_j \rangle + \langle u_j^2 \rangle \approx 2\langle u_i^2 \rangle \tag{8}$$

where u_i are the individual zonal velocities. With decorrelated velocities, the relative diffusivity, $K^{(2)}$, is constant and equal to twice the absolute diffusivity, $K^{(1)}$ (the time derivative of the absolute dispersion; see Sec. 2).

Relative dispersion is the second moment of pair displacements, but more fundamental statistically is the probability density function (PDF) of the displacements; given the PDF, one may calculate all moments (e.g. Mandel, 1984). Relative dispersion in both an energy and an enstrophy cascade produces non-Gaussian PDF's (Richardson, 1926; Sullivan, 1971; Bennett, 1987). Non-Gaussian PDF's are usually indicative of organized flow, and decorrelated pair velocities conversely are expected to produce Gaussian PDF's (Bennett, 1987). So the PDF is potentially an important measure for assessing the character of relative dispersion.

b. Previous dispersion observations

Richardson (1926) famously first measured relative dispersion by observing smoke spreading from smokestacks. His results were consistent with a relative diffusivity

which increased with distance and was proportional to distance to the 4/3 power, as in (3).

Similar behavior has been observed at the ocean surface. Richardson and Stommel (1948) and Stommel (1949) used parsnips, flourescine dye and paper cards to deduce an approximate $D^{4/3}$ dependence for the diffusivity at scales from 50 cm to 100 m. Okubo (1971) examined the spreading of dye from various experiments, primarily in the North Sea, and found the 4/3 law for dispersion on scales 100 m to 100 km. Similar results were found also by Anikiev *et al.* (1985).

Davis (1985) calculated relative diffusivities as a function of distance using surface drifters in the California current. His diffusivities increased up to about 30 km, but did not exhibit a power law dependence on distance and moreover appeared to change in time. The reason for the difference with the previously mentioned results is unknown.

In the 1970's there were two large experiments in the atmosphere in which balloons were launched in pairs. In the first (the EOLE experiment, at 200 mb), the mean square pair separation increased exponentially in time early on and linearly in time thereafter, or at scales exceeding 1000 km (Morel and Larcheveque, 1974). Were the atmosphere a 2D turbulent fluid, this would imply an enstrophy cascade below an energy-containing scale of order 1000 km. Exponential growth was also detected in the second experiment (the TWERLE experiment, at 150 mb) at early times, but the subsequent growth was faster-than-linear, and perhaps as fast as t^3, up to 10,000 km (Er-El and Peskin, 1981). The authors suggested a transition from an enstrophy to an energy inertial range (the reason for the discrepancy with Morel and Larcheveque is unclear, but may be related to a mean shear; see Bennett (1987) and Sec. 4c).

Relative dispersion calculations using data from the subsurface ocean are rare. Jim Price calculated relative diffusivities using SOFAR float data from the Local Dynamics Experiment (LDE; Rossby *et al.,* 1986b) in the western North Atlantic (a figure he made is shown in McWilliams *et al.,* 1983). Price found that $K^{(2)} \propto D^n$ where $4/3 \leq n \leq 2$, from scales of roughly ten to several hundred kilometers.

Likewise, few investigators have calculated relative displacement PDF's, and even those results are somewhat mixed. Sullivan's (1971) measurements of dye spreading at the surface of Lake Huron produced Gaussian PDF's for displacements over hundreds of meters. But the surface drifters described by Davis (1985) exhibited a non-Gaussian distribution soon after deployment and normal statistics later on (suggesting pair velocities were correlated only initially). Er-el and Peskin (1981) similarly found non-normal distributions five days after the deployment of the TWERLE balloons, or during the period of exponential growth; however, they did not check the distributions later on.

c. Present work

We will examine relative dispersion with subsurface float data. Data from the Local Dynamics Experiment will be re-examined, and augmented by data from the Site L experiment (Price *et al.,* 1987). New data will also be analyzed, from the eastern and

central Atlantic (A Mediterranean Undercurrent Seeding Experiment or AMUSE; Bower *et al.,* 1997; Hunt *et al.,* 1998; and the Atlantic Climate Change Experiment or ACCE; Bower *et al.,* 1999) and from the northwestern Atlantic (the North Atlantic Current or NAC experiment; Zhang *et al.,* 2000). A number of floats in these experiments were deployed in pairs and, though the sample size is still modest by theoretical standards (Babiano *et al.,* 1990), this is the best one can do at present.

2. Data and methods

Our trajectories come from subsurface floats. These are neutrally buoyant subsurface drifters, ballasted for a specific pressure or density surface and tracked acoustically using the deep sound channel. Position fixes, as well as temperature and pressure measurements, were made from 1–3 times per day (e.g. Rossby *et al.,* 1986a).

The float trajectories are shown in Figure 1. The boxes in the figure indicate four regions to be discussed, that of the AMUSE experiment in the east, the LDE (Rossby *et al.,* 1986b) and Site L experiments in the west, the NAC experiment in the northwest and the ACCE experiment in the east/central region. Pairs were sought in other data sets too, but no other yielded as many as these five sets.

Both the Site L and LDE experiments had floats at 700 m in the same region, so those data were grouped together (and referred to as the "Site L set"). There are additional floats at 1300 m from the LDE set, and they will be treated separately (the "LDE1300 set"). The ACCE and NAC regions overlap, but the latter has a greater concentration of floats near the western boundary.

The floats used in the AMUSE, LDE and Site L experiments were isobaric or constant depth, but those in the NAC and ACCE experiments were quasi-isopycnal[2] and thereby occupied a range of depths. The current thinking is that isobaric and isopycnal floats behave similarly outside boundary currents (Davis, 1991). Of course, a number of floats in the NAC and Site L regions *are* in boundary currents. However, a recent statistical analysis which included both isobaric and isopycnal floats, including the NAC and Site L floats, showed no systematic differences (LaCasce, 2000). So no distinction is made between the different float types (see also Sec. 2a).

The first task is to identify float pairs. A pair is taken to be any two floats which come within a predefined distance at a given time. Thus "chance pairs" are used in addition to those deployed together ("original pairs"), which effectively doubles the sample size in some of the sets. The same tactic was employed by Morel and Larcheveque (1974) and Er-el and Peskin (1981), and neither found systematic differences between the pair types.

Three different maximum separations were used for identifying pairs: 7.5, 15 and 30 km. The smaller the maximum initial separation, the greater the range of scales sampled, but

2. The floats have a piston which permits them to change their compressibility, which in turn makes them approximately neutrally buoyant.

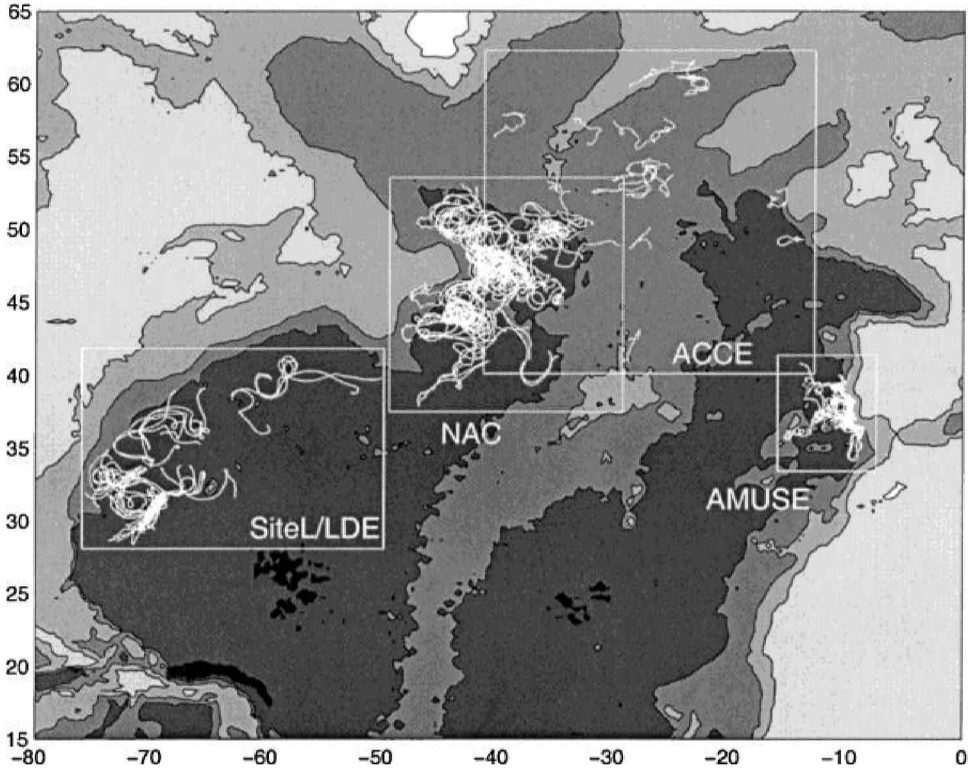

Figure 1. Pair trajectories used in this work. The boxes indicate the individual experiments which are, from right to left, AMUSE, ACCE, NAC and Site L/LDE. Note the LDE1300 and Site L sets are in the same box; the former are mostly in the cluster in the lower left portion of the box. These represent 50 day segments of longer float trajectories.

also the smaller the sample size. The numbers of pairs as a function of initial separation are tabulated in Table 1.

As can be seen, the AMUSE set has the most pairs and the LDE1300 the fewest. The other three sets have comparable numbers. Note the temporal resolution of the data was one day in most cases, but 8 hours for the AMUSE data and 12 hours for the NAC data. The quasi-isopycnal NAC floats were deployed on two density surfaces, $\sigma = 27.2$ and $\sigma = 27.5$ (typically 200 m apart), and only pairs of floats on the same density surface were used.

Once a pair was located, the zonal and meridional separations were calculated for a fixed number of days (50). Taking a uniform record length like this makes for smoother averages, but necessitated discarding a few "chance" pairs which came into range near the end of one of the float's lifetimes. Including those partial segments did not change the results, within errors.

After the pairs were identified, we calculated various quantities. The mean square

Table 1. Float experiments with numbers of pairs. The numbers of pairs as a function of initial separation are shown in the second through fourth columns. In the fifth are the total number of 50 day trajectory segments in the area (see Fig. 9). The temporal resolution is shown in the sixth, and the rms zonal/meridional velocities (units m/sec) in the seventh.

Experiment	Depth	$D_0 \leq 7.5$	$D_0 \leq 15$	$D_0 \leq 30$	50 day	δt (days)	rms (u/v), $D_0 \leq 15$
AMUSE	1000 m	28	54	89	122	1/3	.060/.060
ACCE	400–800 m	14	22	50	616	1	.055/.051
NAC	100–900 m	19	38	81	105	1/2	.31/.32
Site L (+LDE)	700 m	14	33	75	222	1	.10/.083
LDE1300	1300 m	4	14	37	62	1	.054/.068

separation is the dispersion; one may define the dispersion tensor (Batchelor, 1952) thus:

$$\langle D_{ij}^2(t)\rangle \equiv \frac{1}{N}\sum_{\text{pairs}} y_i(t)\, y_j(t) \tag{9}$$

where y_i is the separation in the zonal ($i = 1$) or meridional ($i = 2$) direction and N is the number of pairs. The trace of this matrix is the "total" relative dispersion:

$$\langle D^2\rangle \equiv \langle D_{11}^2\rangle + \langle D_{22}^2\rangle. \tag{10}$$

For comparison, the absolute (single particle) dispersion is defined:

$$\langle X_{ij}^2(t)\rangle \equiv \frac{1}{M}\sum_{\text{particles}} (x_i(t) - \langle x_i(t)\rangle)(x_j(t) - \langle x_j(t)\rangle), \tag{11}$$

where x_i is the particle displacement from its initial position and M the number of particles. Single particle dispersions were also calculated; no mean flow corrections were made (Davis, 1991), but mean flow effects will be discussed.

Assuming the relative displacements are normally distributed, the 90% confidence limits for the dispersion are defined as (e.g. Mandel, 1984):

$$\langle D_{ij}^2(t)\rangle \left(1 \pm z\left\langle\frac{2}{N}\right\rangle^{1/2}\right) \tag{12}$$

with $z = 1.65$ (assuming N is sufficiently large). Most sets have displacement statistics which are nearly Gaussian (Sec. 3h), so such confidence limits are reasonable.

Given the relative dispersion, one can define a relative diffusivity:

$$K_{ij}^{(2)}(t) \equiv \frac{1}{2}\frac{d}{dt}\langle D_{ij}^2(t)\rangle; \tag{13}$$

similarly $K^{(1)}$, the single particle diffusivity, is the derivative of the absolute dispersion, given in (11). We calculated the diffusivities by center-differencing the dispersions.

We will also examine the mean square relative speeds, or:

$$\left\langle \left| \frac{dD_i}{dt}(t) \right|^2 \right\rangle \equiv \frac{1}{N} \sum_{\text{pairs}} \left| \frac{d}{dt} y_i(t) \right|^2 , \tag{14}$$

where the single subscript, $i = 1, 2$, indicates displacements in the zonal and meridional directions, respectively. As noted in Section (1a), the mean square relative velocity is twice the mean square particle velocity when pair velocities are uncorrelated. So we normalize the relative velocities in (14) by the latter (see Sec. 3g).

A potential shortcoming of the relative dispersion calculation relates to averaging pairs with a range of separation distances. Given that distance is the fundamental quantity of interest, one could choose instead to make it the independent variable and time the dependent variable. This is the idea behind so-called finite scale Lyapunov exponents (FSLE's), in use recently in the study of chaotic and turbulent flows (Benettin *et al.,* 1980; Aurell *et al.,* 1997; Artale *et al.,* 1997). We calculated FSLE's, but the results broadly supported our dispersion calculations (Appendix).

a. Vertical shear

Vertically-sheared currents can cause horizontal dispersion among floats at different depths. A typical value of the shear in the geostrophic mean in the western North Atlantic at 1000 m depth is 1 mm/sec over 100 m (Roemmich and Wunsch, 1985), so that two floats separated by 100 m of depth will drift roughly 100 m apart over a day. Since typical float velocities are an order of magnitude larger, this is a small difference; in fact, 100 m is smaller than the uncertainty in an individual float position. The shear in the mean in the east is even less (Saunders, 1982).

The mean shear in the Gulf Stream is of course much greater, and can be as much as 10 cm/sec over 100 m at 700 m depth (Johns *et al.,* 1995). There are several instances of floats in the Site L set being entrained by the Gulf Stream; likewise, some floats in the western portion of the NAC region were advected by the North Atlantic Current, which has comparable baroclinic shear (Meinen *et al.,* 2000). So vertical shear may be an issue in the west.

These estimates are for the mean flow, but a better measure would be the shear of the rms velocities. Unfortunately the latter is typically not known with precision (current meters have instruments separated typically by several hundreds of meters), so we can say little about this.

To find evidence of vertical shear effects, we plotted pair trajectories from the western regions alongside of pressure records for the individual floats. Were shear important, one might expect pairs with greater pressure differences to separate faster. But this was not the case. For example, two floats separated by 100 m depth might travel together for 10 days, whereas two within 10 m separate after only 2 days. Furthermore, strong vertical shear would presumedly produce differences between isobaric and isopycnal floats, because the latter are better at tracking fluid parcels; but the results from the NAC and Site L regions

are similar. So we suspect that dispersion due to vertical shear is probably much less than that due to horizontal shear (see also Sec. 4c).

3. Results

The regional results are presented first, beginning in the east and working westward. In each region, the results are displayed in one figure, with the following format (e.g. Fig. 2): in the upper left panel are the components of the relative dispersion tensor for the pairs with $D_0 \leq 15$ km, the zonal and meridional as well as the cross term, $\propto y_1 y_2$, with their 90% confidence limits. In the upper right panel are the absolute dispersions for the corresponding individual floats with their 90% confidence limits. And in the lower panel are the total relative diffusivities as a function of distance for the three maximum initial separations (along with the absolute diffusivity, $K^{(1)}$, multiplied by two, for comparison).

a. AMUSE

The floats in the AMUSE experiment lie just off the Iberian coast, in the eastern North Atlantic (Fig. 1). The floats were deployed in the Mediterranean outflow, frequently in pairs and occasionally in triplets. Most were between 1000 and 1200 m depth, but a few were shallower, at 700 m depth. Nearly identical results were obtained with and without the 700 m floats (consistent with weak vertical shear), so the latter were included.

The zonal and meridional relative dispersions (Fig. 2, upper left panel) exhibit nonlinear initial growth, followed by approximately linear growth after 10 to 15 days. The cross relative dispersion is decreasing slightly, but is mostly not different from zero. The absolute dispersions (right upper panel) appear to grow linearly in time after only the first few days.

The meridional relative dispersion is more than twice the zonal dispersion (and significantly different). The absolute dispersion is also meridionally anisotropic, although less so. Note too that the meridional relative dispersion is larger than its absolute counterpart.

This meridional anisotropy can be contrasted the *zonal* anisotropy of the (absolute) dispersion in the nearby interior found by Spall *et al.* (1993), or the weak diagonal anisotropy in the NW-SE direction described by Ollitrault and Colin de Verdiere (2000). The present anisotropy can be traced to floats moving northward along the Iberian coast. Recalculating the dispersion using only chance pairs in the interior yields a dispersion which is statistically isotropic (although why it is not zonally- or diagonally-enhanced is not known).

The total (zonal + meridional) diffusivities are shown in the lower panel for the three maximum initial separations, and are plotted against $\langle D \rangle$, the mean distance.[3] For all separations, the diffusivity increases up to a scale of roughly 50 km; it is approximately constant thereafter and equal roughly to twice the absolute diffusivity. The absolute

3. Bennett (1987) reminds us that $\langle D^2 \rangle^{1/2} \neq \langle D \rangle$ and that potential differences exist using one or the other. We plotted diffusivity against both quantities but obtained nearly identical results.

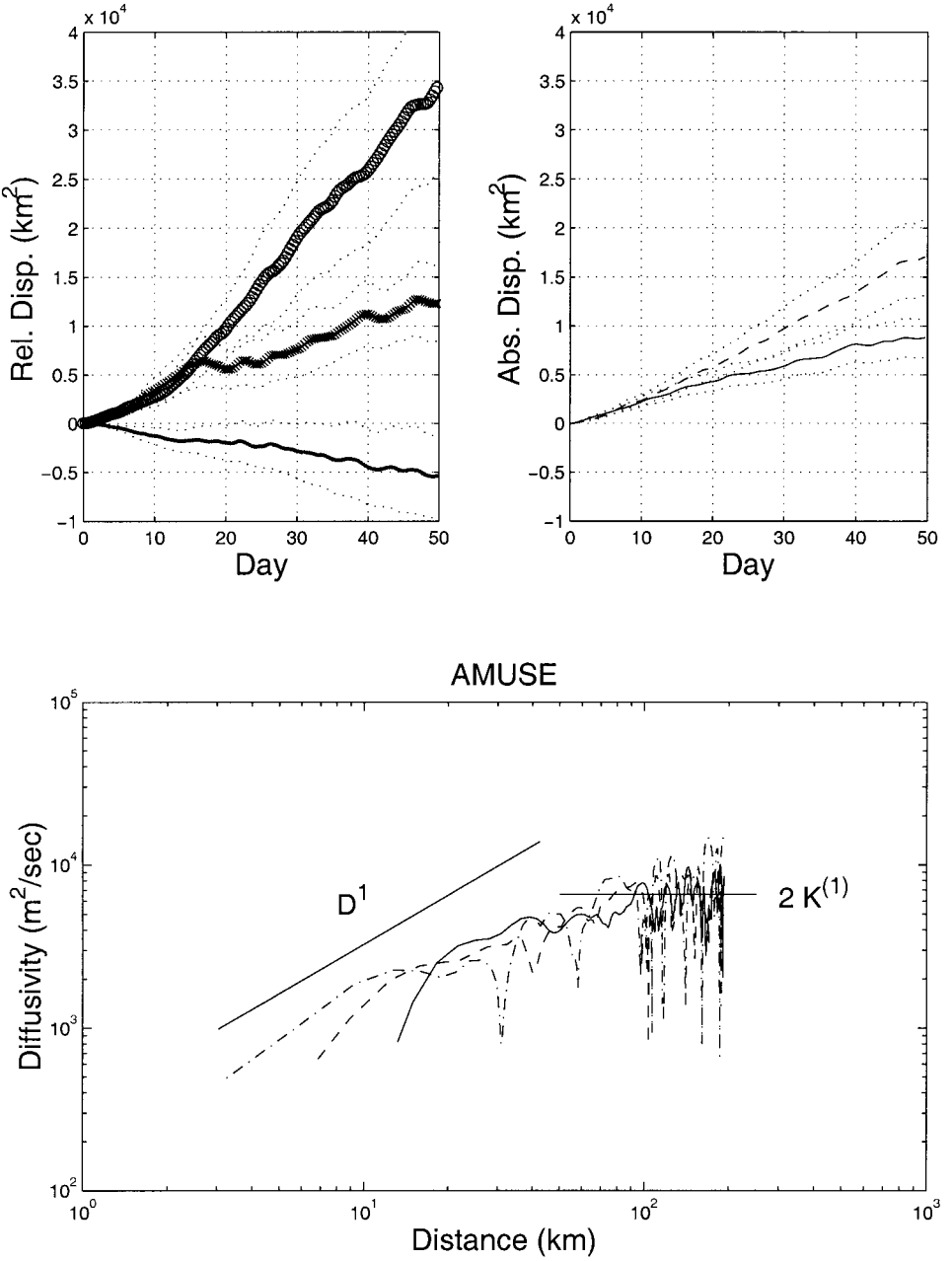

Figure 2. Statistics in the AMUSE experiment. In the upper left panel are the relative dispersions in the zonal (x), meridional (o) directions as well as the cross zonal/meridional dispersion (.). The 90% confidence limits are indicated by the small dots. In the upper right panel are the single particle dispersions in the zonal (solid) and meridional (dashed) directions for the individuals in the pairs. At the bottom are the relative diffusivities vs. mean separation distance for various maximum initial separations: $D_0 \leq 7.5$ km (dash-dot), $D_0 \leq 15$ km (dashed) and $D_0 \leq 30$ km (solid). The dots indicate twice the absolute dispersion for the individuals plotted against the rms distance from the starting position.

diffusivity (calculated with linear fits to the dispersion curve and its errors) is $3.3 \pm 0.8 \times 10^3$ m^2/sec, which compares reasonably well with the zonal diffusivity in the interior of $K_{11} = 2.1 \times 10^3$ m^2/sec of Spall *et al.* (1993) and with the isotropic diffusivity in the Canary Basin of 1.7×10^3 m^2/sec of Ollitrault and Colin de Verdiere (2000).

At small scales, the diffusivities exhibit an approximate power law dependence, with $K^{(2)} \propto D^n$, with $2/3 \leq n \leq 1$. The increase is definitely less than either $D^{4/3}$ from (3), or D^2 from (6). Because the diffusivities do not level off before 50 km or more, one sees similar behavior with all three maximum initial separations.

b. ACCE

The ACCE region is in the central North Atlantic, straddling the mid-Atlantic ridge (Fig. 1). The sets contains many floats but few pairs, yielding a smaller sample size than in the AMUSE set.

The dispersion results (Fig. 3) are noisier but broadly similar to those in the AMUSE region. Both relative and absolute dispersions increase linearly in time (within error) after roughly 10 days, and the cross term is zero. Note the dispersion is isotropic, and that relative and absolute dispersions are of similar magnitude. This is different than with the full AMUSE set, but similar to the interior portion of the latter (not shown).

The relative diffusivities for all initial separations increase to roughly 50 km and, though noisy, level off at larger scales. They are comparable to twice the absolute diffusivity at large scales, which is $2.8 \pm 0.8 \times 10^3$ m^2/sec or about the same as in the AMUSE region. At small scales the diffusivity scales approximately as D^1, like in the AMUSE region.

c. NAC

The NAC floats are in the Newfoundland Basin, that is, between the Grand Banks and the mid-Atlantic ridge (Fig. 1). The North Atlantic Current and its associated eddies dominate the flow (Zhang *et al.,* 2000), and the region is richly energetic.

A striking aspect here (Fig. 4) is that the relative dispersion is substantially greater than in the previous sets (see also Fig. 7 below), reflecting much more vigorous stirring. And while the absolute dispersion appears to increase linearly after 5–10 days, the relative dispersion exhibits nonlinear growth over most of the 50 days. As before, the relative dispersion cross term is not different from zero.

Both the relative and absolute dispersion are isotropic. With a strong boundary current nearby, it is perhaps curious that this is so; judging from the trajectories, it appears that the floats in these pairs did not remain long near the boundary, but instead veered off into the basin interior (Fig. 1). In fact, this may explain why vertical shear appears to be relatively unimportant here (Sec. 2a and Sec. 4c).

The relative diffusivities also are much larger than in the previous sets but, interestingly, the increase of diffusivity with distance is faster than before and is consistent with a $D^{4/3}$ dependence. Moreover, the scale at which the diffusivity levels off, roughly 100–200 km, is larger than in the previous sets, implying larger energy-containing eddies. At the largest

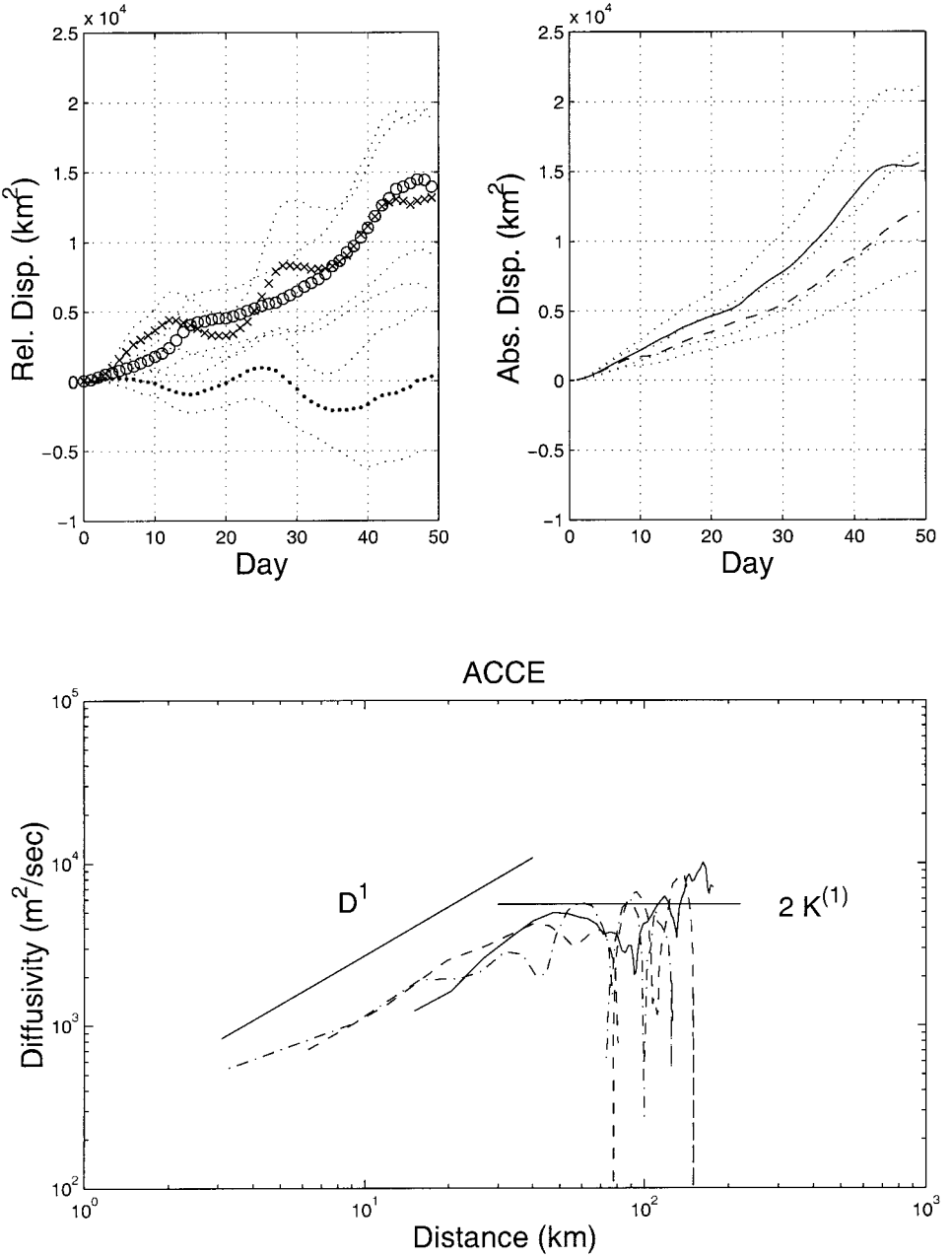

Figure 3. Statistics for the ACCE set. See Figure 2 for details.

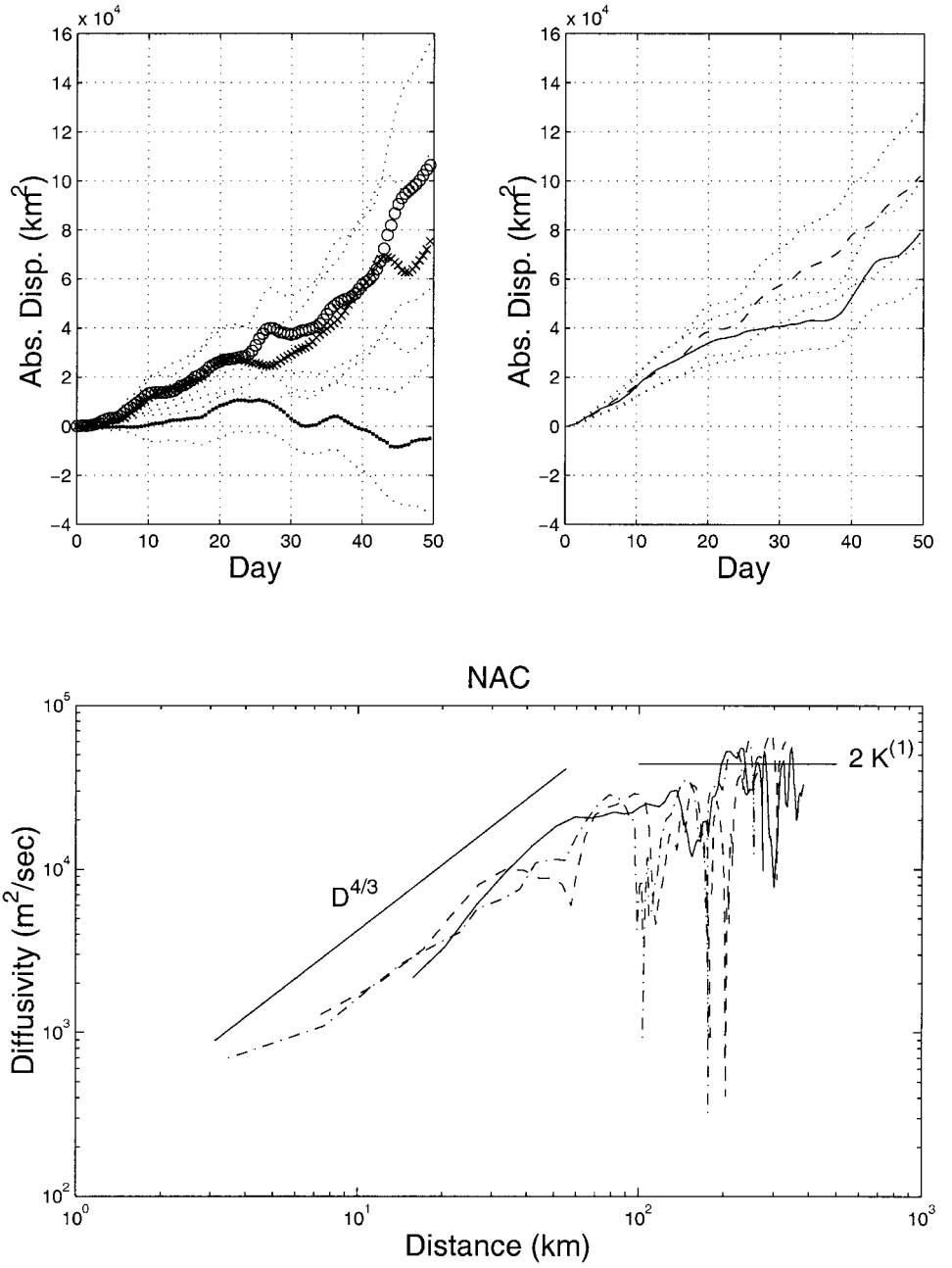

Figure 4. Statistics for the NAC set. See Figure 2 for details.

scales, the relative diffusivity is roughly equal to twice the absolute diffusivity, which is $2.2 \pm 0.75 \times 10^4$ m^2/sec.

d. Site L and LDE 700

The Site L and LDE floats are to the south, and south of the mean position of the Gulf Stream (Fig. 1). This is another region known to be rich in eddies. Some floats translate rapidly eastward, presumedly under the influence of the Gulf Stream, but most are not so obviously affected.

The relative and absolute dispersions are comparable to those from the NAC region (Fig. 5). Like with the NAC set, the zonal and meridional relative dispersion exhibit nonlinear growth, at least until about day 20; thereafter, the growth is approximately linear. Different from the NAC set is that the absolute dispersion is three times greater in the zonal direction than in the meridional. This may imply large scale zonal advection.[4] Again, the cross relative dispersion term is not different from zero.

The relative diffusivities are roughly constant at scales greater than 100–200 km, but somewhat less than twice the absolute diffusivity due to the large zonal absolute diffusivity. The (total) absolute diffusivity at large scales is roughly $1.6 \pm 0.6 \times 10^4$ m^2/sec, somewhat less than in the NAC region. But as with the NAC pairs, the Site L diffusivity increases approximately as $D^{4/3}$ at scales smaller than 100 km.

e. LDE 1300

The last set contains floats in the same region but 600 m deeper, below the main thermocline. This set has the smallest number of pairs and hence noisier statistics, but is included nevertheless for comparison.

The relative dispersion increases over the 50-day period and is isotropic (Fig. 6). The absolute dispersion is similarly isotropic, within the errors.

Interestingly, the cross term of the relative dispersion *is* significantly different from zero after day 30, suggesting zonal and meridional velocities are correlated. Examining the trajectories, one finds that most of the floats were moving back and forth along an axis tilted with the horizontal. The apparent cause was a 300 km scale Rossby wave which advected floats back and forth across f/H contours, which are similarly tilted (Price and Rossby, 1982).

One can eliminate the correlation by calculating the relative dispersions with respect to rotated coordinate axes. It turns out the cross term vanishes with a (counterclockwise) axis rotation of about 45 degrees, which is approximately perpendicular to the f/H lines. Under this rotation the relative dispersion is no longer isotropic, but instead greatest *across* f/H contours (see also Section 4d).

The relative diffusivity increases over the range of scales sampled (up to roughly 100 km), although the relative diffusivity at late times is highly uncertain. The $D_0 \leq 30$ km

4. Unlike relative dispersion, absolute dispersion is not Gallilean invariant.

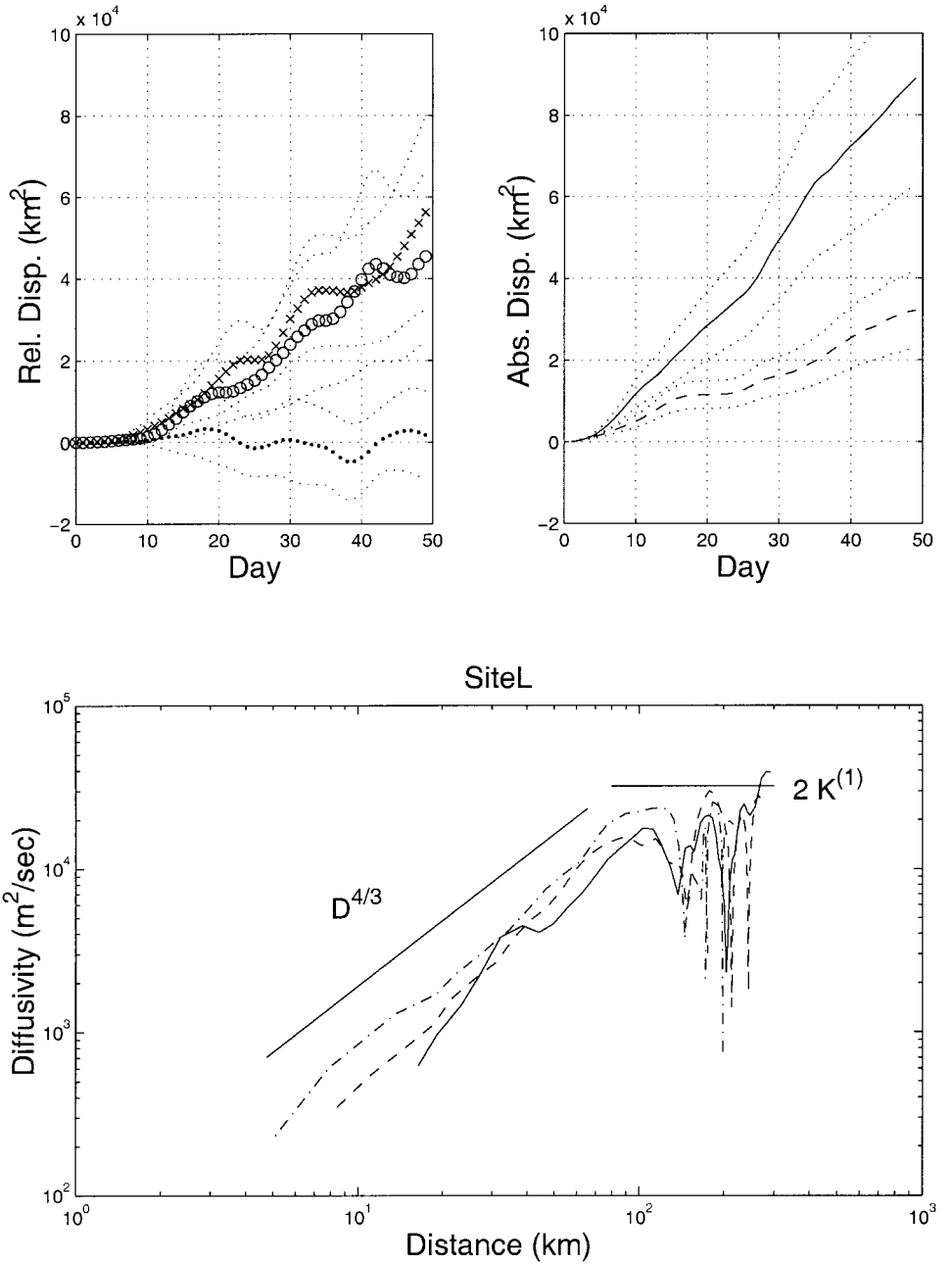

Figure 5. Statistics for the Site L set. See Figure 2 for details.

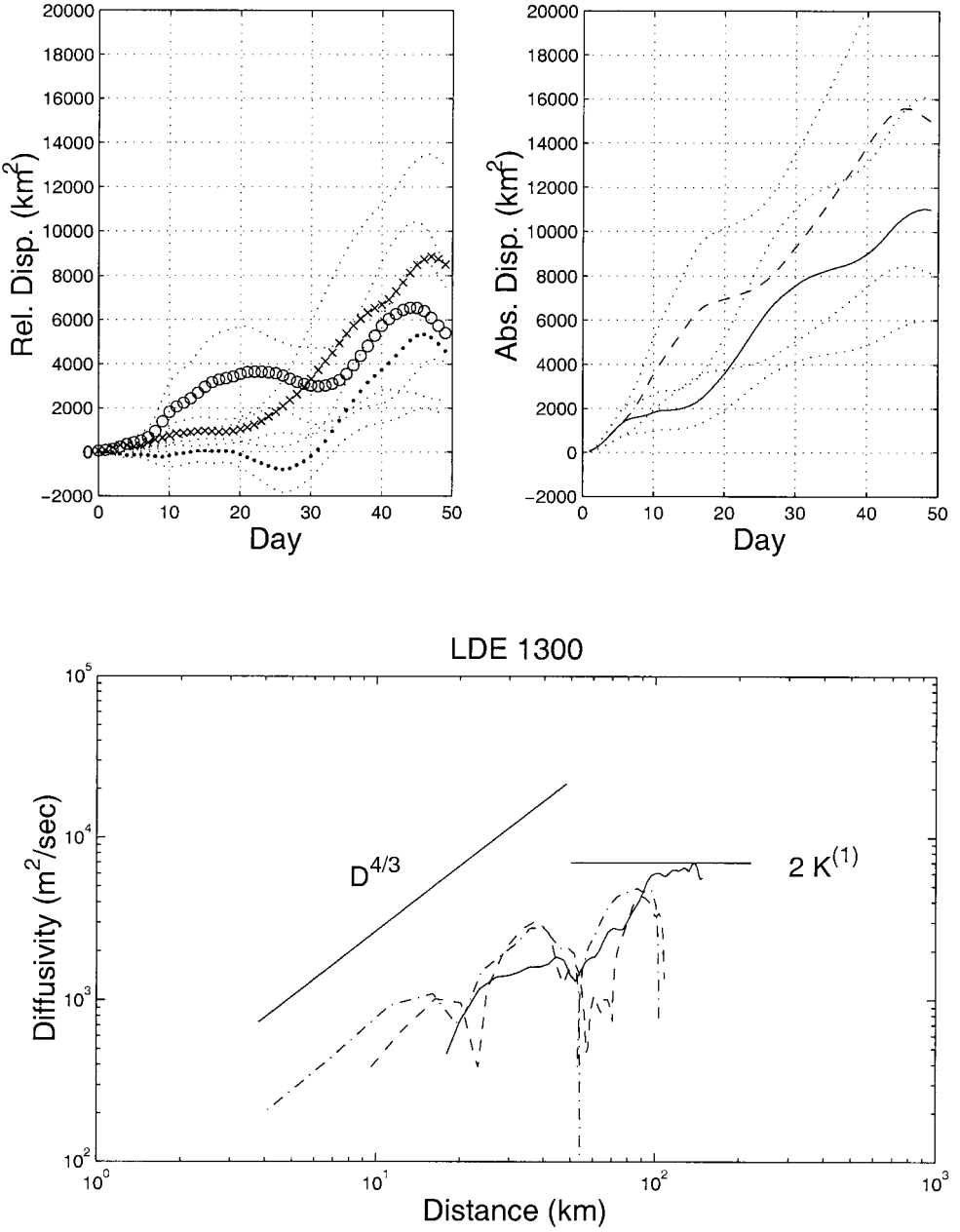

Figure 6. Statistics for the LDE 1300 set. See Figure 2 for details.

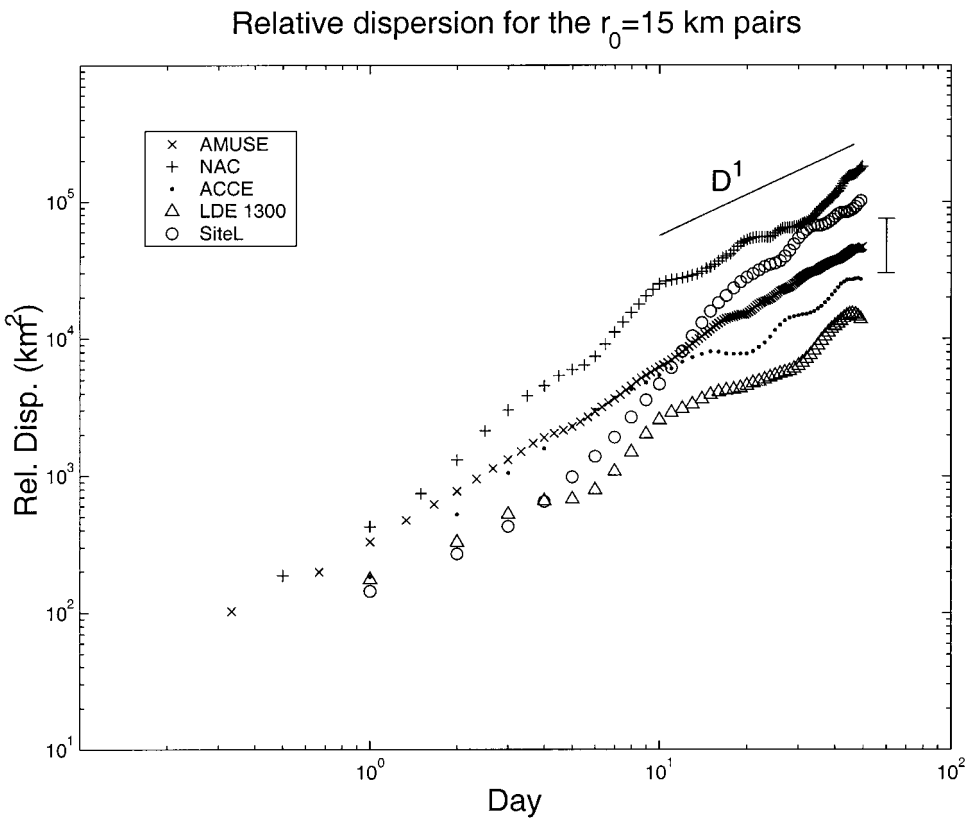

Figure 7. The total relative dispersion with $D_0 \leq 15$ km for all experiments. The 90% confidence limits for the ACCE set are indicated by the bars.

diffusivity reaches a value somewhat less than twice the absolute diffusivity, but it's not clear it has leveled off. The absolute diffusivity is roughly $3.5 \pm 1.5 \times 10^3$ m^2/sec, or somewhat less than at 700 m, but comparable to that in the AMUSE and ACCE regions. The diffusivities do not exhibit a simple power law behavior, but the growth appears somewhat less than $D^{4/3}$.

f. Comparing dispersion

To examine regional variations, we now consider the five sets together; log-log plots of the total relative dispersion for all the $D_0 \leq 15$ km pairs are shown in Figure 7. The error bars indicate the 90% confidence limits for the ACCE set, and give a rough idea of the uncertainties in the other sets.

The results in all cases are broadly consistent with nonlinear initial growth followed by linear growth, with a transition at around 10 days. The major difference is in the magnitudes of dispersion, with much greater spreading occurring in the two western sets.

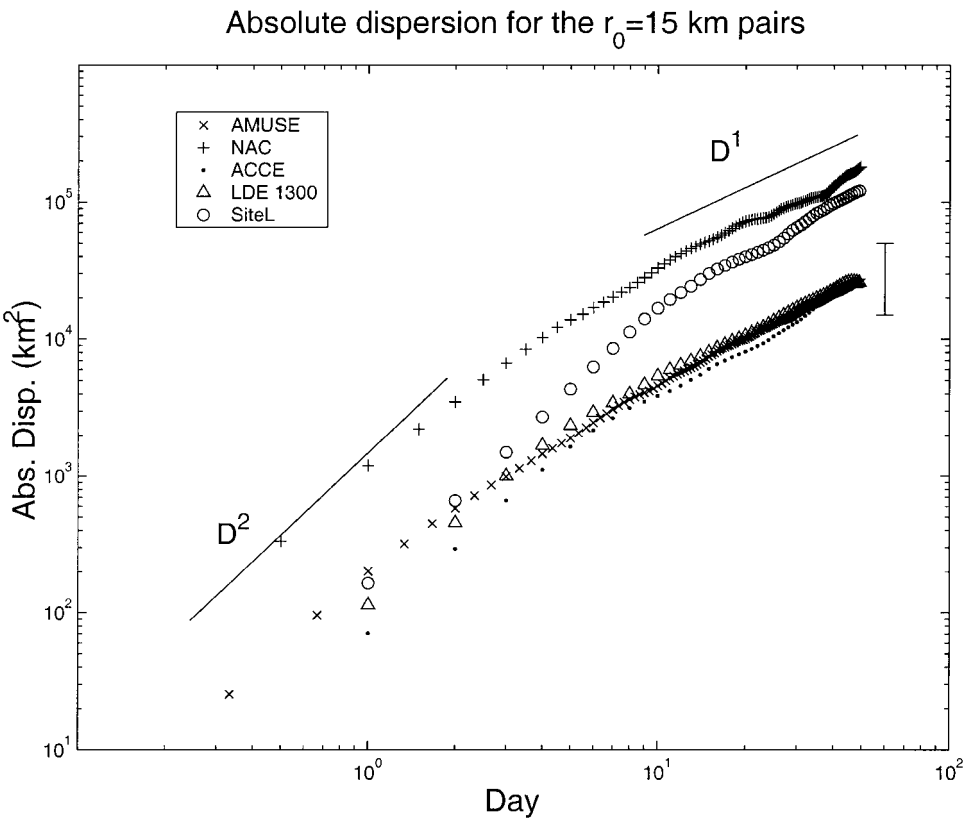

Figure 8. The single particle dispersions for the individuals used in Figure 7. Quadratic and linear growth rates are indicated by the lines.

The Site L group stands out, with its slow initial growth followed by an explosive increase between 5 and 20 days. The NAC pairs experience a similarly violent growth, but spread out over a longer period, from a half day to 10–20 days.

The absolute dispersions for the individuals in the $D_0 \leq 15$ km pairs are shown in Figure 8. Here too, one finds similar behavior among the sets which moreover fits the classical description: an initial growth quadratic in time followed by linear growth, with a transition occurring around the Lagrangian integral time (e.g. Batchelor and Townsend, 1953). The Site L set again stands out, with an intermediate "anomalous" phase; this may reflect the influence of elliptical flow structures, like vortices (Elhmaidi *et al.,* 1993). However a similar phase is not found with the NAC pairs, which also lie in an eddy-rich region.

Curiously, the ACCE, AMUSE and LDE1300 sets have essentially identical absolute dispersions (and, therefore, diffusivities). This is somewhat surprising, given the difference in locations and depths. But then the pairs may not be representative of their respective regions. To address this, the absolute dispersions were found for *all* floats from each

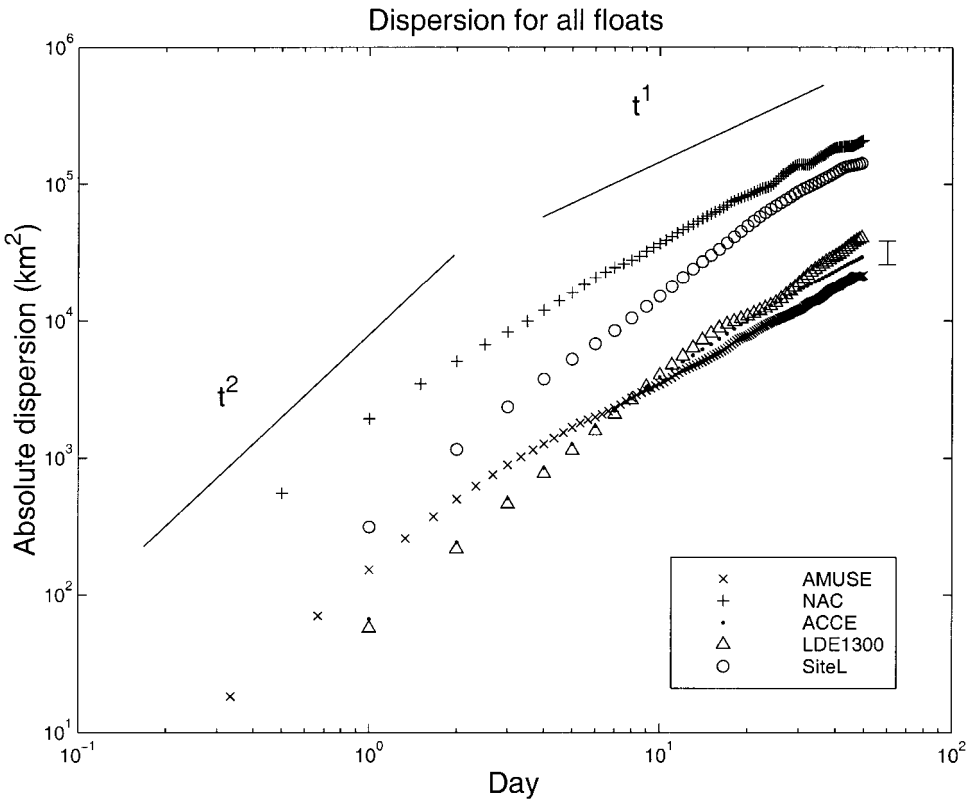

Figure 9. The single particle dispersions for all floats in the respective regions. The trajectories have been cut into 50-day segments for this calculation. Note the sample sizes are greater in this case, which is reflected by the smaller (ACCE) error bars.

experiment (not just the pairs). All trajectories were broken into 50-day segments which were treated as statistically independent (a reasonable assumption, given the Lagrangian time scale is less than 20 days everywhere). The numbers of segments are shown in column 5 of Table 1. The absolute dispersion curves, with the ACCE 90% confidence limits are shown in Figure 9. Note the latter are smaller than those in Figure 8 because there is more data here.

The general agreement between Figures 8 and 9 suggest the pairs are in fact representative. However, there are notable differences. For one, the dispersion is slightly different in the AMUSE, ACCE and LDE1300 sets, with greater dispersion occurring as one moves east to west; this is perhaps more sensible than having the same dispersion in the three regions, given what we know about the eddy energy distribution in the North Atlantic (e.g. Wunsch, 1981).

Secondly, the absolute dispersion in the LDE1300 set mirrors that in the Site L set. In fact, multiplying the LDE1300 dispersion by four yields a curve *indistinguishable* from the

Site L dispersion curve. Both exhibit the "anomalous" growth seen in Figure 8 for the Site L floats. Of course, similar absolute dispersion does not imply similar relative dispersion, but it is at least possible the relative dispersion at 1300 m and 700 m could have been more alike had we had more pairs at 1300 m.

But for these differences, Figures 8 and 9 essentially agree. In addition, the zonal/meridional anisotropy for each of the larger sets mimics that seen for the pairs, suggesting the pair results are representative in that regard too.

g. Mean relative velocities

As a further comparison, we also examined the mean relative velocities. The motivation here is to discover whether pair velocities are correlated and/or accelerating at any time (Sec. 1a).

Plotted in Figure 10 are the zonal and meridional mean square relative velocities from each set. As noted earlier, each component has been normalized by twice the single particle velocity variance in the same direction; a value of one suggests decorrelated pair velocities, from Eq. (8), assuming the flow is (locally) homogeneous.

In the AMUSE set, the normalized velocities oscillate about 1 the entire time. The same is approximately true for the ACCE set. So the pair velocities are decorrelated over most of the 50-day period for both sets. (This is not inconsistent though with relative dispersions growing over the first 10 days; see Sec. 4a).

The Site L and NAC sets in contrast exhibit a growth in relative velocities over the first 10 days and possibly longer, indicating accelerating pair velocities; thereafter the normalized variances are near unity. Notice that the NAC pairs exhibit a more rapid acceleration over the first 10 days, which may be related to the difference in relative dispersion from the Site L set seen in Figure 8.

Strangest of all is the LDE1300 set, in which the velocities have variances well below unity *for the whole period.* As noted in Section 3e, the LDE1300 relative diffusivities never quite level off, which also is consistent with correlated velocities. But unlike the Site L or NAC cases, there is little hint of acceleration. The relative velocities with respect to coordinate axes rotated by 45 degrees (not shown) similarly never reach unity, but the velocity in the direction across f/H shows greater variance than that along.

h. Displacement distributions

Lastly, we consider the pair displacement PDF's. As noted in Sec. 1a, non-Gaussian PDF's may indicate organized flow, and such PDF's are found with either an energy or an enstrophy cascade (Bennett, 1987). The kurtosis (the fourth order moment) is a common means of characterizing the shape of a PDF; Gaussian distributions have a kurtosis of three, and larger kurtoses indicate extended "wings" (an excess of outliers).

Histograms of the displacements were found for all sets and at all times during the 50-day period, and the kurtoses calculated (Fig. 11). To correct for lateral inhomogeneities, one should normalize the displacements using local (binned) rms velocities (see Bracco *et*

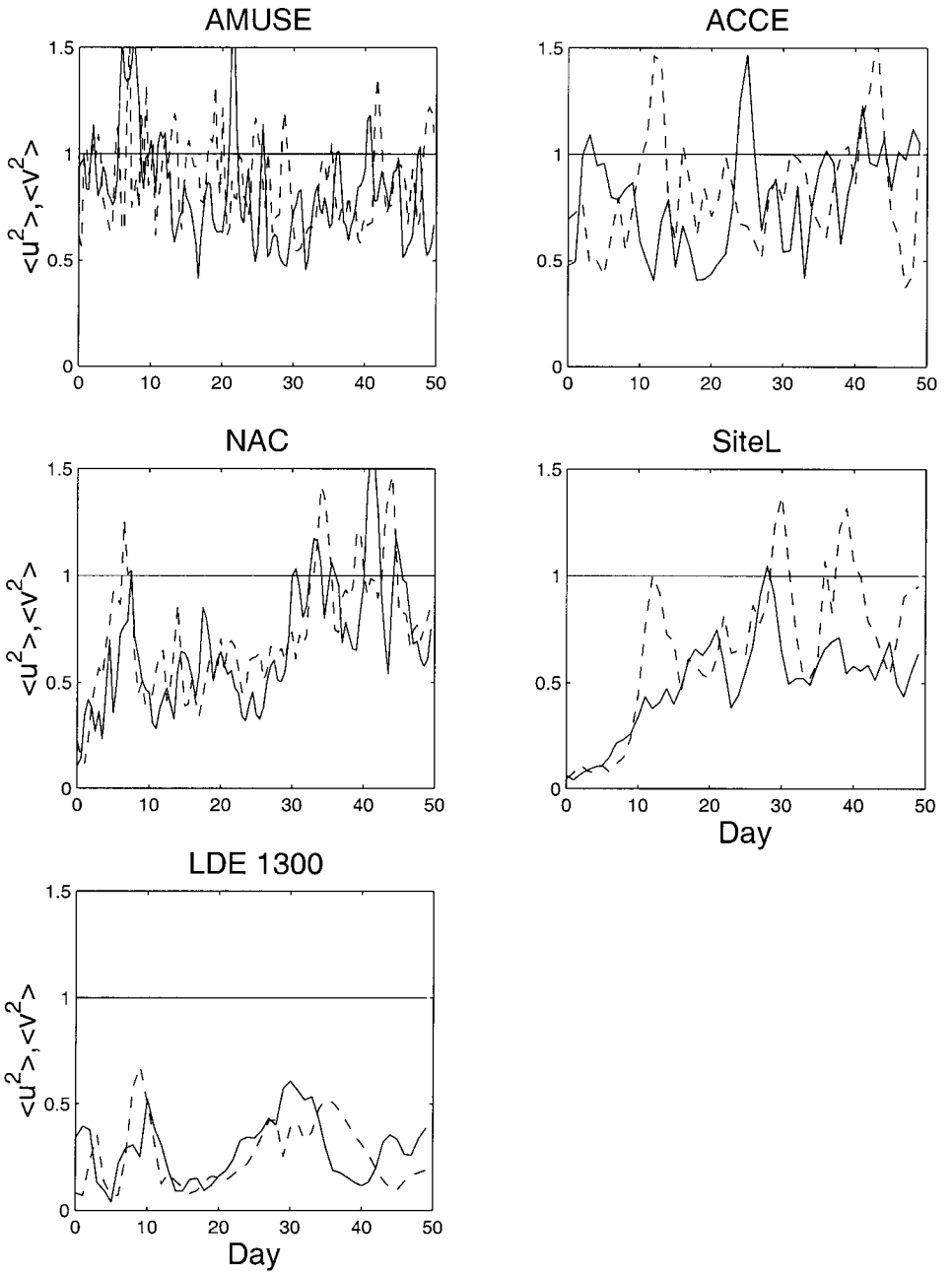

Figure 10. The relative zonal and meridional velocity variances vs. day for all cases. The variances have been normalized by twice the single particle variances, so a value of unity indicates the relative velocities are decorrelated.

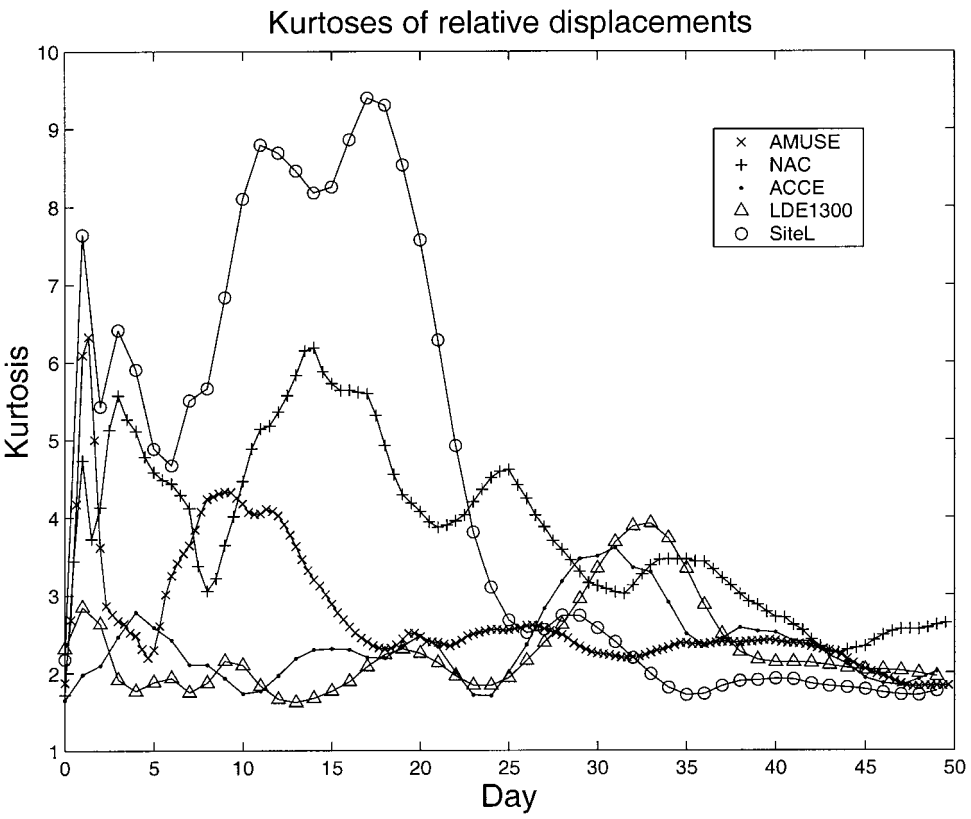

Figure 11. The kurtoses of the relative displacements versus time for all sets. Note a value of three corresponds to a Gaussian distribution.

al., 2000); we did not do so. But the trajectories in all five cases lie in relatively compact regions; such normalization would be necessary if one were to calculate kurtoses for all the sets combined.

The results in Figure 11 are somewhat noisy, but the general pattern is clear. The AMUSE, ACCE and LDE1300 kurtoses are not significantly different from three for nearly the entire period, though the AMUSE kurtoses are somewhat elevated in the first days. In contrast, the NAC and particularly the Site L sets exhibit larger kurtoses during the first 20 days, before falling to three thereafter. The relevance of this is discussed below.

It's worth noting that a kurtosis *near* 3 does not guarantee decorrelated velocities. The LDE1300 kurtoses are generally near 2, but the relative velocity variances (Sec. 3g) are less than one, which is counter to expectation for decorrelated velocities. In fact the LDE1300 distributions are closer to a uniform than a Gaussian distribution, and the former has a kurtosis just less than 2.

4. Discussion

How do the present results compare with theoretical predictions? We address this by considering relative dispersion in several idealized cases, as follows.

a. Stochastic mixing

What if float advection were simply a stochastic process? Consider a simple Markov model of particle advection, in which the Lagrangian acceleration is a combination of decay and white noise:

$$du_i = -\frac{1}{T_i} u_i dt + n_i dW, \tag{15}$$

where T_i is the Lagrangian time scale, n_i a noise amplitude and dW an incremental Wiener process (e.g. Sawford, 1993; Griffa *et al.,* 1995). Particles in such cases exhibit "classical" absolute dispersion: an initial growth proportional to t^2 followed by a linear growth after the Lagrangian integral time (Batchelor and Townsend, 1953). The absolute diffusivities thus grow as D^1 initially and are constant at larger scales, with the transition occurring at $L_E \equiv \langle u_i \rangle T_i$ (the product of the rms velocity and the Lagrangian time scale). Because particle velocities are uncorrelated in space, the relative velocity variances equal twice the absolute velocity variances *at all times,* that is, even during the initial period. And presuming the "noise" is Gaussian, the pair displacements will be normally distributed.

The eastern sets (AMUSE and ACCE) exhibit behavior along these lines. The relative velocities are essentially decorrelated at all times, and the diffusivities increase like D^1 initially and are constant at late times. One difference is that the relative dispersion is twice the absolute dispersion at late times for the stochastic case, and while this is apparent for the meridional dispersion in the AMUSE set (Fig. 2), it is not for the zonal dispersion nor for the ACCE dispersions (Fig. 3). Taking errors into account though, a factor of two difference is plausible.

Because L_E is proportional to the rms velocity, more energetic flows have larger energy-containing scales. This then is consistent with larger scales in the west (Table 1). However, because the western relative velocities are correlated initially and the growth of diffusivity with distance too rapid, we suspect the stochastic explanation is insufficient there.

b. 2-D Turbulence

i. Initial growth. Were the ocean like homogeneous 2-D turbulence locally, we would expect certain dispersive behavior (Sec. 1a). For one, the initial temporal growth of the dispersion in either an enstrophy or an energy cascade would be quadratic in time. Babiano *et al.* (1990) show:

$$\langle D^2 \rangle \approx D_0^2 + 2S(D_0)t^2 \qquad \text{as } t \to 0 \tag{16}$$

where $S(D_0)$ is the second order Eulerian structure function, and suggest such growth can persist up to the Lagrangian integral time, which is proportional to the inverse square root of the mean enstrophy (Babiano *et al.,* 1987).

The Lagrangian integral time in all cases is on the order of days, but is somewhat longer in the east than in the west (approximately 10 and 5 days, respectively); so there is a greater chance of seeing such initial growth in the east. A quadratic growth of dispersion implies diffusivity grows linearly with both time and distance, and such was seen for the ACCE set and possibly the AMUSE set. Again though, the ACCE and AMUSE relative velocities were apparently decorrelated at all times, which is not consistent. So the agreement in the growth in diffusivity with distance may be fortuitous.

The relative velocities were apparently correlated for the western sets, where plots of pair dispersion versus time can also be fit approximately with quadratics over the first few points. However this is uncertain and greater temporal resolution would be required to say for sure.

ii. Turbulent enstrophy cascade. At longer times, the pair statistics will depend on whether there is an energy or an enstrophy cascade over the scales sampled. Assuming an energetic peak at scale L_E, it is plausible that enstrophy is cascading to smaller scales. Were this the case, relative diffusivities would grow as $\langle D^2 \rangle$ and relative velocities increase exponentially in time. While we cannot rule out such a rapid growth in the relative velocities in any set, the diffusivities clearly increase more slowly than D^2 everywhere. Moreover, if exponential stretching is occurring, the "characteristic time," defined:

$$\tau(t) = \frac{\langle D^2(t) \rangle}{K^{(2)}(t)}$$

will be constant during the given interval (Babiano *et al.,* 1990). It was not so in any of the present five cases. As a further test we calculated "Finite Scale Lyapunov Exponents" (FSLE's) for the sets, but found no evidence for exponential growth there either (Appendix).

A possible explanation is that the initial pair separations are too large relative to the energy-containing scale, L_E. The exponential growth phase is not observed until the dependence on the initial separation, D_0, is lost (Babiano *et al.,* 1990) and by that time the pair separations may have already reached L_E. The relative displacement kurtoses are elevated over the first few days for the AMUSE pairs (Fig. 11), which may be consistent with a cascade; however no similar indication is seen with the ACCE pairs. Elevated kurtoses are found for the western sets, but the growth in diffusivity is more suggestive of an energy cascade (see below).

So the question of an enstrophy cascade in the eastern and central regions remains open. We would point out though that the dye released in the North Atlantic Tracer Release Experiment (in the east) was stretched into filaments in a manner consistent with exponential stretching (Ledwell *et al.,* 1998). But further studies with closer float pairs are required to know for sure.

iii. Turbulent energy cascade. A second possibility is that energy is cascading to larger scales, driven by a source at small scales. Then diffusivities would increase as $D^{4/3}$ until the scale at which the cascade ceases (Sec. 1a). From (4), the relative velocity variances would increase linearly in time and the relative dispersion would grow as t^3 (Richardson, 1926; Batchelor, 1952). In addition, the displacement kurtoses would likely be non-Gaussian (Bennett, 1987).

Such behavior apparently occurs with the Site L/LDE 700 m and NAC pairs. In particular, the diffusivities exhibit a growth proportional to $D^{4/3}$ from roughly 10 to 100–200 km in both regions. In both cases also the relative velocities are accelerating and the kurtoses elevated initially (although the acceleration and the corresponding growth in dispersion is apparently faster with the NAC pairs; Fig. 7). In addition, indirect evidence for a t^3 growth in dispersion in both regions was found with the FSLE's (Appendix).

If an energy cascade is occurring in the west, the likely sources would be the baroclinically unstable Gulf Stream and North Atlantic Current, both of which could "inject" energy near the deformation radius (Salmon, 1980). Energy would cascade up to L_E, which our results suggest is 100–200 km. Why does it stop there? One possibility is that dissipation (most likely bottom friction) limits the cascade, but alternately, the cascade may *arrest* due to competition from planetary waves (Rhines, 1975). The arrest scale is roughly $(U/\beta)^{1/2}$, or about $(0.2/2 \times 10^{-11})^{1/2} \approx 100$ km. We know that arrested geostrophic turbulence is usually strongly zonally anisotropic (Rhines, 1975), whereas the Site L and NAC relative dispersions are isotropic (Fig. 5); but the absolute dispersion at Site L *is* zonally anisotropic, which may be related.

If there were a cascade to large scales, it ought to be significantly barotropic (Salmon, 1980), implying that the response at 1300 m in the LDE region should resemble that at 700 m. While the relative dispersion at the two depths appeared to be different, the absolute dispersion using all floats in the region was almost the same (albeit of smaller amplitude at 1300 m; Sec. 3f). As discussed below, the LDE1300 statistics in many ways are consistent with wave advection, as suggested by Price and Rossby (1982). This is interesting because an arrested turbulent flow can look exactly like a wave from the Lagrangian perspective (LaCasce and Speer, 1999). If so, the arrested wave would have an advective speed comparable to its phase speed, and in fact this is so: from Price and Rossby (1982), the wave phase speed was about 6 cm/s, a value comparable to the rms velocity in Table 1. So the LDE1300 results are (perhaps!) also consistent with arrested geostrophic turbulence.

As discussed above, we were unable to rule out an enstrophy cascade in the east because pairs too quickly reached the energy-containing scale, L_E. The same applies to an energy cascade; it could be happening in the east, but due to the insufficient separation between D_0 and L_E, the asymptotic limit in which (3) obtains never occurs. An energy cascade in the east would require a source at subdeformation scales, but this too is possible.

Again, we found elevated kurtoses during the initial growth phase with the Site L and NAC sets. Were an inverse cascade occurring, this would be at odds with Sullivan (1971) who found nearly normal distributions from dye measurements. Given the present results,

one wonders if he might have seen elevated kurtoses had he looked sooner after the dye injection. Elevated kurtoses are predicted by the model of turbulent diffusion proposed by Richardson (1926).

c. Shear advection

The 4/3 law can also appear with mixing in the presence of a background shear (Bowden, 1965; Bennett, 1987). With a zonal mean shear, particles undergoing a random walk in the meridional direction will have (Bennett, 1987):

$$\langle (y - y_0)^2 \rangle = 4K_y t, \qquad \langle (x - x_0)(y - y_0) \rangle = 2K_y \left\langle \frac{dU}{dy} \right\rangle t^2$$
$$\text{and} \qquad \langle (x - x_0)^2 \rangle = x_0^2 + \frac{4}{3} K_y \left\langle \frac{dU}{dy} \right\rangle^2 t^3, \tag{17}$$

where K_y is the meridional diffusivity. The t^3 growth in the zonal dispersion is accompanied by a $D^{4/3}$ growth in the zonal diffusivity.

Bennett suggested that shear may have been behind the t^3 growth seen by Okubo (1971; see Sec. 1b), because Okubo's length scales greatly exceed those expected for the 3D turbulence inertial range. Similarly, shear dispersion may explain the difference between the results of Er-el and Peskin (1981) and Morel and Larcheveque (1974), because, as noted by Er-el and Peskin, the mean shear at 150 mb is not negligible.

Given that the Site L and LDE experiments lie on the southern flank of the Gulf Stream, it's plausible the Gulf Stream shear is responsible for the observed $D^{4/3}$ dependence. Likewise, the sheared NAC could be behind the 4/3 growth in the Labrador Basin. That the zonal single particle dispersion was far greater than the meridional at Site L (Fig. 5) also may indicate mean advection.

However, other points differ. The relative dispersion in both Figures 5 and 4 is isotropic. Isotropy is perhaps possible if the mean is not zonal and mixing is occurring in both directions, but the cross term for the relative dispersion was zero, suggesting no correlation between zonal and meridional separations. From (17), the cross dispersion should increase more rapidly than the dispersion across the mean shear. Indeed, neither the Site L or NAC pairs show much evidence of a mean shear. Some pairs translate parallel to the jets, but more move obliquely or even counter to them (Fig. 1).

A second possibility is that the floats experience significant vertical shear. Vertical shear could produce a $D^{4/3}$ growth in the lateral diffusivity with laterally isotropic relative dispersion. Of course, the 4/3 dependence was found with both the quasi-isopycnal floats in the NAC and the isobaric floats at Site L, which argues against a role for vertical shear. However, it must be admitted that either vertical or horizontal shear may impact our results in the west.

d. Wave advection

Another type of shear advection can occur with planetary waves. A particle advected by a monochromatic Rossby wave loops but also drifts, and the magnitude and direction of the drift vary with both the latitude and longitude of particle deployment (Flierl, 1981). As such, a group of particles experiences quadratic dispersion in the direction of the wave phase speed (LaCasce and Speer, 1999). With meridional mixing superimposed, the dispersion could in principle increase as t^3, exactly as with a simple shear.

To test this idea, a kinematic wave model like that used in LaCasce and Speer (1999) was employed in conjunction with the stochastic advection scheme prescribed in Eq. (15) (and used in LaCasce, 2000) to advect a group of particles. Consistent with the previous statements, the relative dispersion in the zonal direction (parallel to the wave phase speed) increased like t^3 (not shown). Like in (17), the meridional dispersion grew only linearly in time. The normalized mean square relative velocities were less than unity in both directions for many wave periods (because the drift velocity is much less than the typical "looping" velocity).

Several features of the LDE1300 set are consistent with this picture: the normalized relative velocity variances are less than unity and a $D^{4/3}$ dependence of the total diffusivity cannot be ruled out.

But other points do not fit so well. The cross relative dispersion vanishes when the coordinate axes are rotated by about 45 degrees (Sec. 3e), an angle similar to that between local f/H and the latitude lines. But then the relative dispersion is greatest in the direction *perpendicular* to local f/H rather than parallel to it, and the dispersion parallel to f/H is essentially constant in time in the final 20 days. This is exactly opposite to expectation.

The plane wave model may be too simple for this region; far from being a collinear field, f/H here is curved with a scale of curvature not much greater than the loops which the floats execute. Alternately we could calculate the dispersion of displacements relative to the f/H field itself, as LaCasce (2000) did with the absolute dispersion and f/H. But this is beyond the present scope.

5. Summary and conclusions

Pair statistics were calculated for subsurface floats in the North Atlantic. Pair dispersion and the implied scale of the energy-containing eddies are both greater in the west than in the east. In addition, floats tend to travel together longer in the west, which produces a quantitative difference in the initial growth of the dispersion. Exponential stretching was not resolved in any region.

The results are in many ways consistent with predictions from the theory of 2-D turbulence. That the relative diffusivity scales as the separation to the 4/3 power in the west is consistent with 2-D turbulence in which energy is cascading to large scales. The dispersion in the east *may* also be consistent with either an energy or an enstrophy cascade, but the spatial resolution of the data there prevent us from determining this.

A second possibility concerns stochastic mixing. The results from the eastern sets are like those obtained under simple Markovian advection, and those in the west could be explained by stochastic mixing superimposed on a mean shear, either horizontal or vertical. As discussed in Section 4c, several details are at odds with such an interpretation, but we cannot rule it out. Of course there is the question of the origin of the mixing (which might simply be temporally unresolved 2-D turbulent dispersion).

The present results derive from modest numbers of float pairs, and the uncertainties are large. Our understanding would benefit greatly from future float experiments designed specifically to measure pair separation. For one, this might settle the question of exponential growth of pair separations. And relative dispersion near the Gulf Stream deserves greater scrutiny, both in and below the main thermocline.

Acknowledgments. The work was supported by NSF grant OCE-9616952. JL gratefully acknowledges fruitful discussions with Breck Owens and Jim Price (who were thinking of relative dispersion when designing the LDE and Site L experiments). We're grateful to Tom Rossby and his colleagues for the NAC floats, many of which were also deployed in pairs. JL discussed FSLE's with Guido Boffetta and Guglielmo Lacorata. Michel Ollitrault and Huaimin Zhang made useful comments on an early version of the manuscript. Detailed comments by an anonymous reviewer were also very helpful. This is Woods Hole Oceanographic contribution number 10196.

APPENDIX

FSLE's

An alternate means of measuring dispersion is to take distance as the independent variable and time as the dependent variable. To do this, we select a set of separations, related thus:

$$y_n = Ry_{n-1} = R^n y_0. \tag{18}$$

where R is a number greater than one. Then we measure the time required for pair separations to grow from y_n to y_{n+1}, defined T_n, and those times are averaged. Written in the form:

$$\lambda(y_n) \equiv \frac{1}{\ln(R)}\left\langle\frac{1}{T_n}\right\rangle, \tag{19}$$

the average approximates the maximum Lyapunov exponent in the limit of small bin spacing (Aurell *et al.,* 1997).

When particle divergence is exponential, the time required for the separation distance to double is constant, and the FSLE too is constant. Alternately, if the relative dispersion obeys a power law,

$$D^2 \propto t^n, \tag{20}$$

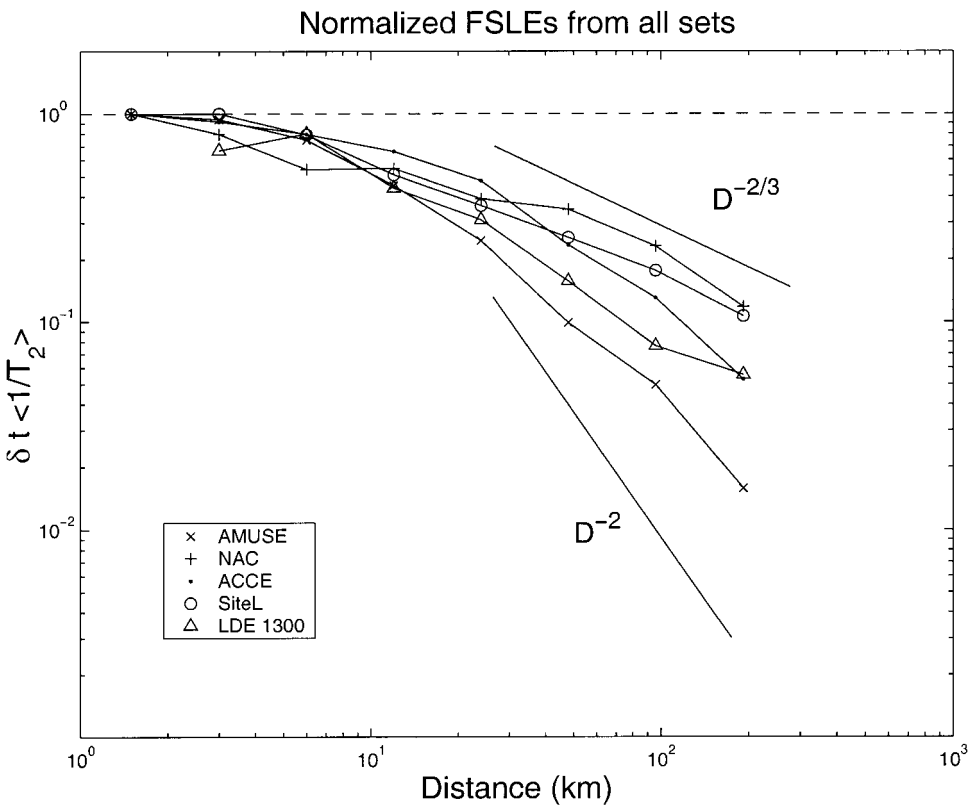

Figure 12. The Finite Size Lyapunov Exponents (FSLE's) for all sets. The mean separation times have been normalized by each set's time step, δt, so a value of unity indicates the doubling time is equal to the time step.

then the FSLE has the corresponding behavior:

$$\langle 1/T_n \rangle \propto y^{-2/n}. \tag{21}$$

In contrast to the relative dispersion, *all* pairs are used for the FSLE, regardless of their closest distance; each pair only contributes to the mean of T_n corresponding to the y_n spanned.

FSLE's were calculated for the five previously-discussed sets. Usually the FSLE is normalized by the logarithm of the scaling factor, R, as in (19), but I chose to normalize by the temporal spacing of the data, so that the maximum value of $\langle 1/T_n \rangle$ would be one. The y_n were calculated using $R = 2$, but the results do not depend on this choice.

The FSLE's are shown in Figure 12. In all cases, the mean inverse doubling time decreases with distance. Most curves plateau at scales less than a few kilometers, but the plateau occurs at $\langle 1/T_n \rangle = 1/(\Delta t)$, which means only that growth at these distances is not

temporally resolved. Surprisingly, this applies even to the AMUSE data, where floats were located every eight hours.

As noted in Section 1a, a linear growth in the relative dispersion would cause $\langle 1/T_n \rangle$ to decrease like D^{-2}. The slopes at larger separations are somewhat difficult to assess, but are generally somewhat less than D^{-2}. The Site L and NAC sets exhibit the slowest rate of decline, with a dependence like $D^{-2/3}$; the latter is consistent with a growth in dispersion which is cubic with time (and $K^{(2)} \propto D^{4/3}$).

Comparing with the dispersion curves from the previous sections does reveal discrepancies, for example, the Site L and NAC curves never decrease like D^{-2}; but the differences stem from the way the two measures are calculated. For one, all pairs nearer than the largest bin separation are used, so there is more data at large scales. Second, the FSLE identifies the first time at which separations exceed a given scale and so is discrete, not continuous. And lastly, the FSLE time is really a *difference* in times.

Nevertheless, these results broadly support our previous findings suggesting that, at least in these cases, averaging distances at discrete times was not problematic.

REFERENCES

Anikiev, V. V., O. V. Zaytsev, T. V. Zaytseva and V. V. Yarosh. 1985. Experimental investigation of the diffusion parameters in the ocean. Izv. Atmos. Ocean Phys., *21,* 931–934.

Artale, V., G. Boffetta, A. Celani, M. Cencini and A. Vulpiani. 1997. Dispersion of passive tracers in closed basins: beyond the diffusion coefficient. Phys. Fluids A, *9,* 3162–3170.

Aurell, E., G. Boffetta, A. Crisianti, G. Paladin and A. Vulpiani. 1997. Predictability in the large: an extension of the concept of Lyapunov exponent. J. Phys. A: Math. Gen., *30,* 1–26.

Babiano, A., C. Basdevant, P. LeRoy and R. Sadourny. 1987. Single-particle dispersion, Lagrangian structure function and Lagrangian energy spectrum in two-dimensional incompressible turbulence. J. Mar. Res., *45,* 107–131.

—— 1990. Relative dispersion in two-dimensional turbulence. J. Fluid Mech., *214,* 535–557.

Basdevant, C., B. Legras, B. Sadourny and M. Beland. 1981. A study of barotropic model flows; intermittency waves and predictability. J. Atmos. Sci., *38,* 2305–2326.

Batchelor, G. K. 1952. Diffusion in a field of homogeneous turbulence, II; the relative motion of particles. Proc. Cambridge Philo. Soc., *48,* 345–362.

—— 1960. The Theory of Homogeneous Turbulence, Cambridge University Press, 197 pp.

—— 1969. Computation of the energy spectrum in homogeneous two-dimensional turbulence. Phys. Fluids Supp. II, *12,* 233–239.

Batchelor, G. K. and A. A. Townsend. 1953. Turbulent Diffusion. Surveys in Mechanics, *23,* 352–398.

Benettin, G., L. Galgani, A. Giorilli and J. M. Strelcyn. 1980. Lyapunov characteristic exponents for smooth dynamical systems and for Hamiltonian systems: a method for calculating all of them. Meccanica, *15,* 9.

Bennett, A. F. 1987. A Lagrangian analysis of turbulent diffusion. Rev. of Geophys., *25*(4), 799–822.

Bowden, K. F. 1965. Horizontal mixing in the sea due to a shearing current. J. Fluid Mech., *21,* 83–95.

Bower, A. S., L. Armi and I. Ambar. 1997. Lagrangian observations of meddy formation during A Mediterranean Undercurrent Seeding Experiment. J. Phys. Oceanogr., *27,* 2545–2575.

Bower, A. S., P. L. Richardson and H. D. Hunt. 1999. Warm water pathways in the northeastern North Atlantic. EOS, Trans. Amer. Geophys. Union, *80*(17), S181.

Bracco, A., J. H. LaCasce and A. Provenzale. 2000. Velocity pdfs for oceanic floats. J. Phys. Oceanogr., *30,* 461–474.

Davis, R. E. 1985. Drifter observations of coastal surface currents during CODE: the statistical and dynamical view. J. Geophys. Res., *90,* 4756–4772.

—— 1991. Observing the general circulation with floats. Deep-Sea Res., *38*(Suppl.), S531–S571.

Elhmaidi, D., A. Provenzale and A. Babiano. 1993. Elementary topology of two-dimensional turbulence from a Lagrangian viewpoint and single-particle dispersion. J. Fluid Mech., *257,* 533–558.

Er-el, J. and R. Peskin. 1981. Relative diffusion of constant-level balloons in the Southern hemisphere. J. Atmos. Sci., *38,* 2264–2274.

Flierl, G. R. 1981. Particle motions in large-amplitude wave fields. Geophys. Astrophys. Fluid Dyn., *18,* 39–74.

Griffa, A., K. Owens, L. Piterbarg and B. Rozovskii. 1995. Estimates of turbulence parameters from Lagrangian data using a stochastic particle model. J. Mar. Res., *53,* 371–401.

Guckenheimer, J. and P. Holmes. 1983. Nonlinear Oscillations, Dynamical Systems, and Bifurcations of Vector Fields, Springer-Verlag, 459 pp.

Hunt, H. D., C. M. Wooding, C. L. Chandler and A. S. Bower. 1998. A Mediterranean Undercurrent Seeding Experiment (AMUSE): Part II. RAFOS Float Data Report May 1993–March 1995. WHOI Technical Report WHOI-98-14, Woods Hole Oceanographic Institution, Woods Hole, MA. 123 pp.

Johns, W. E., T. J. Shay, J. M. Bane and D. R. Watts. 1995. Gulf Stream structure, transport and recirculation near 68W. J. Geophys. Res., *100,* 817–838.

Kraichnan, R. H. 1966. Dispersion of particle pairs in homogeneous turbulence. Phys. Fluids, *9,* 1937–1943.

—— 1967. Inertial ranges in two-dimensional turbulence. Phys. Fluids, *10,* 1417–1423.

Kolmogorov, A. N. 1941. The local structure of turbulence in incompressible viscous fluid for very large Reynolds number. Dokl. Akad. Nauk. SSSR, *30,* 9–13.

LaCasce, J. H. 2000. Floats and f/H. J. Mar. Res., *58,* 61–95.

LaCasce, J. H. and K. Speer. 1999. Lagrangian statistics in unforced barotropic flows. J. Mar. Res., *57,* 245–275.

Ledwell, J. R., A. J. Watson and C. S. Law. 1998. Mixing of a tracer in the pycnocline. J. Geophys. Res., *103,* 21499–21529.

Lin, J. T. 1972. Relative dispersion in the enstrophy-cascading inertial range of homogeneous two-dimensional turbulence. J. Atmos. Sci., *29,* 394–396.

Mandel, J. 1984. The Statistical Analysis of Experimental Data, Dover Publications, 410 pp.

McWilliams, J. C., E. D. Brown, H. L. Bryden, C. C. Ebbesmeyer, B. A. Elliot, R. H. Heinmiller, B. Lien Hua, K. D. Leaman, E. J. Lindstrom, J. R. Luyten, S. E. McDowell, W. Breckner Owens, H. Perkins, J. F. Price, L. Regier, S. C. Riser, H. T. Rossby, T. B. Sanford, C. Y. Shen, B. A. Taft and J. C. van Leer. 1983. The local dynamics of eddies in the western North Atlantic, *in* Eddies in Marine Science, Springer-Verlag, 609 pp.

Meinen, C. S., D. R. Watts and R. A. Clarke. 2000. Absolutely referenced geostrophic velocity and transport on a section across the North Atlantic Current. Deep-Sea Res. I, *47,* 309–322.

Morel, P. and M. Larcheveque. 1974. Relative dispersion of constant-level balloons in the 200 mb general circulation. J. Atmos. Sci., *31,* 2189–2196.

Obhukov, A. M. 1941. Energy distribution in the spectrum of turbulent flow. Izv. Akad. Nauk. SSR, Ser. Geogr. Geofiz., *5,* 453–466.

Okubo, A. 1971. Oceanic diffusion diagrams. Deep-Sea Res., *18,* 789–802.

Ollitrault, M. and A. Colin de Verdiere. 2000. SOFAR floats reveal mid-latitude intermediate North Atlantic general circulation. J. Phys. Oceanogr. (submitted).

Pedlosky, J. 1987. Geophysical Fluid Dynamics, Springer-Verlag, 710 pp.

Price, J. F., T. M. McKee, W. B. Owens and J. R. Valdes. 1987. Site L SOFAR float experiment, 1982–1985. Woods Hole Oceanographic Institution Technical Report, WHOI-, WHOI-97-52. 289 pp. (available from http://www.ntis.gov).

Price, J. F. and H. T. Rossby. 1982. Observations of a barotropic planetary wave in the western North Atlantic. J. Mar. Res., *40* (Suppl.), 543–557.

Rhines, P. B. 1975. Waves and turbulence on a beta-plane. J. Fluid Mech., *69,* 417–443.

Richardson, L. F. 1926. Atmospheric diffusion on a distance-neighbourgraph. Proc. R. Soc. London, Ser. A, *110,* 709–737.

Richardson, L. F. and H. Stommel. 1948. Note on eddy diffusion in the sea. J. Meteorol., *5,* 38–40.

Roemmich, D. and C. Wunsch. 1985. Two transatlantic sections: meridional circulation and heat flux in the subtropical North Atlantic. Deep-Sea Res., *32,* 619–664.

Rossby, H. T., D. Dorson and J. Fontaine. 1986a. The RAFOS System. J. Atmos. Oceanic Technol., *3,* 672–679.

Rossby, H. T., J. F. Price and D. Webb. 1986b. The spatial and temporal evolution of a cluster of SOFAR floats in the POLYMODE Local Dynamics Experiment (LDE). J. Phys. Oceanogr., *16,* 428–442.

Rupolo, V., B. L. Hua, A. Provenzale and V. Artale. 1996. Lagrangian velocity spectra at 700 m in the western North Atlantic. J. Phys. Oceanogr., *26,* 1591–1607.

Salmon, R. 1980. Baroclinic instability and geostrophic turbulence. Geophys. Astrophys. Fluid Dyn., *15,* 167–211.

Saunders, P. 1982. Circulation in the North Atlantic. J. Mar. Res., *40* (Suppl.), 641–657.

Sawford, B. L. 1993. Recent developments in the Lagrangian stochastic theory of turbulent dispersion. Boundary Layer Meteor., *62,* 197–215.

Spall, M. A., P. L. Richardson and J. F. Price. 1993. Advection and eddy mixing in the Mediterranean salt tongue. J. Mar. Res., *51,* 797–818.

Stommel, H. M. 1949. Horizontal diffusion due to oceanic turbulence. J. Mar. Res., *8,* 199–225.

Sullivan, P. J. 1971. Some data on the distance-neighbour function for relative diffusion. J. Fluid Mech., *47,* 601–607.

Taylor, G. I. 1921. Diffusion by continuous movements. Proc. Lond. Math. Soc., *20,* 196–212.

Wunsch, C. 1981. Low-frequency variability of the sea, *in* Evolution of Physical Oceanography, B. A. Warren and C. Wunsch, eds., The MIT Press, 342–375.

Zhang, H.-M., M. D. Prater and T. Rossby. 2000. Isopycnal Lagrangian statistics from the North Atlantic RAFOS float observations. J. Geophys. Res., (submitted).

Received: *25 April, 2000;* revised: *25 September, 2000.*